translates vertically upward, and the translational motion is given by

$$y = It/4\rho h - gt^2/2 \qquad \text{(A2)}$$

where g is the acceleration due to gravity.

As discussed, the gap between ring and backup mass for a flyer plate experiment must be large enough to permit free ring deformations. For the ring used in this experiment, a set of trajectory plots of the ring displacements corresponding to several angular positions indicated that for an 80° backup mass a clearance of 0.020 in. per 1000 taps is required between the ring and the top edge of the backup mass.

References

[1] Goodier, J. N. and McIvor, I. K., "Dynamic Stability and Nonlinear Oscillations of Cylindrical Shells (Plane Strain) Subjected to Impulsive Pressure," TR 132, June 1962, Division of Engineering Mechanics, Stanford University, Stanford, Calif.

[2] Forrestal, M. J., Sagartz, M. J., and Walling, H. C., "Comment on Dynamic Response of a Cylinder to a Side Pressure Pulse," *AIAA Journal*, Vol. 11, No. 9, Sept. 1973, pp. 1355–1356.

[3] Bealing, R., "Impulse Loading of Circular Rings," *Experimental Mechanics, Proceedings of the 11th Annual Symposium*, University of New Mexico, 1971, pp. 15–26.

[4] Walling, H. C., Forrestal, M. J., and Tucker, W. K., "An Experimental Method for Impulsively Loading Ring Structures," *International Journal of Solids and Structures*, Vol. 8, 1972, pp. 825–831.

[5] Bealing, R. and Carpenter, P. G., "Exploding Foil Devices for Shaping Megamp Current Pulses," *Journal of Physics E: Scientific Instruments*, Vol. 5, 1972, pp. 889–892.

[6] Sears, F. W. and Zemanski, M. W., *University Physics*, 4th ed., Addison-Wesley, Reading, Mass., 1970, p. 49.

Unsteady Expansion Waveforms Generated by Diaphragm Rupture

J. GORDON HALL,* G. SRINIVASAN,† AND JAIPAL S. RATHI†

State University of New York at Buffalo, Buffalo, N.Y.

IN the theory of ideal shock-tube flow it is customarily assumed that the unsteady expansion wave generated by diaphragm rupture is a perfectly centered plane wave. In practice, however, such waves are generally not centered, or may not even be plane. In some experimental applications the question arises as to how to evaluate or characterize the noncentered waveform. A theoretical model for that purpose was previously introduced in an analysis of unsteady wall boundary layers within noncentered expansion or compression waves.[1,2] The present Note summarizes experimental waveform results obtained by applying the model to wall static pressure histories through expansion waves.

The expansion waves were generated by rapid bursting of a diaphragm (usually 0.003 in. thick mylar) sealing an expansion tube charged with dry room temperature air to pressure p_o (Fig. 1). The tube cross section was $1\frac{1}{2}$ in. by 5 in. The diaphragm was located at the tube end and could be preceded by a $\frac{1}{4}$-in. thick orifice plate giving critical or choked discharge to the room. Controlled initiation of the flow was achieved by electrically heating a wire taped to the stressed diaphragm. Oscilloscope records of wall static pressure vs time through the waves (Fig. 2) were obtained using three Kistler 603-A piezoelectric transducers mounted flush in the center of the 5-in. sidewall at various stations along the tube. Data were obtained to reveal the influence on waveform of orifice-plate geometry, pressure level p_o, and diaphragm material, as well as distance along the tube. Reproducibility of the experiments was extremely good in general.

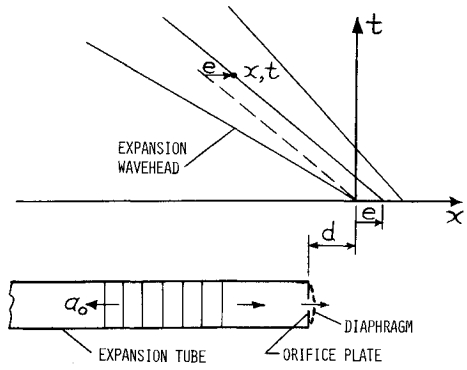

Fig. 1 Expansion tube and straight x, t characteristics for plane noncentered waves.

The theoretical model assumes a plane, isentropic simple wave with one family of the mathematical characteristics being straight lines in the distance-time or x,t plane (Fig. 1). The origin of x,t is located along the wavehead path, as described subsequently, and lies outside the tube at some distance d (typically 1 to 2 ft) from the diaphragm. This representation has no physical reality outside the tube and neglects initial three-dimensional flow effects which occur close to the diaphragm. The model also assumes that the first derivatives of the inviscid flow properties are discontinuous at the wavehead, which requires that the wave be generated with nonzero initial acceleration of the gas. The experimental waves generally had this property to a very good approximation except in the occasional instance of a poor diaphragm rupture. If the wavehead first derivatives are discontinuous it can be shown[2] that they must satisfy the relations $(\partial p/\partial t)_H = a_o(\partial p/\partial x)_H = -2\gamma p_o/(\gamma+1)t$ and $(\partial u_e/\partial t)_H = a_o(\partial u_e/\partial x)_H = -2a_o/(\gamma+1)t$. Here p = pressure, u_e = gas velocity, a = sound speed, γ = specific heat ratio (constant), and subscripts o and H denote conditions ahead of the wave (gas at rest) and at the wavehead, respectively. Thus a wavehead first derivative, such as $(\partial p/\partial t)_H$, measured at any x defines the corresponding time t from these relations and thereby uniquely locates the origin of x,t along the wavehead path. In the case of a centered wave the preceding relations apply not only at the wavehead but throughout the entire centered wave as well.

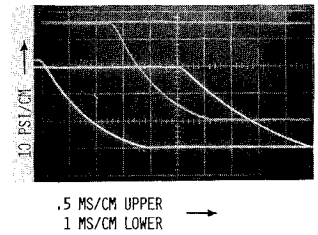

Fig. 2 Typical pressure-time oscilloscope records. Upper beam trace at 2 ft from diaphragm, 0.5 MS/cm sweep. Lower beam traces at 5 ft and 11 ft from diaphragm, 1 MS/cm sweep. p_o = 85 PSI. Choked 1″ × 5″ slot orifice.

Received October 31, 1973. This work was supported by ONR under Contract N000-14-72-C0373.

Index categories: Nonsteady Aerodynamics; Nozzle and Channel Flow.

* Professor, Department of Mechanical Engineering.

† Research Assistant.

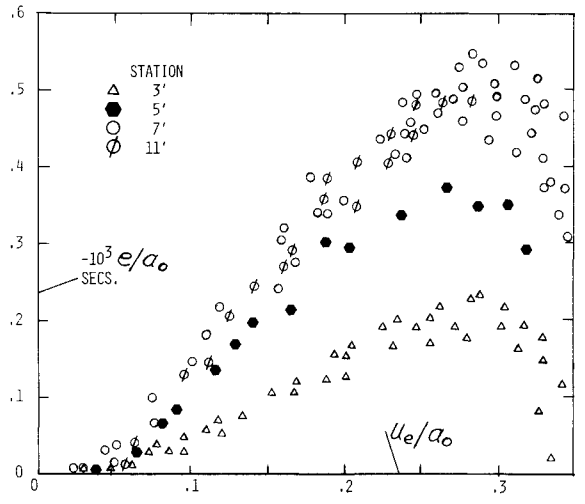

Fig. 3 e **determined from pressure measured at various stations along tube.** $p_o = 85$ **PSI. Choked 1″ × 5″ slot orifice.**

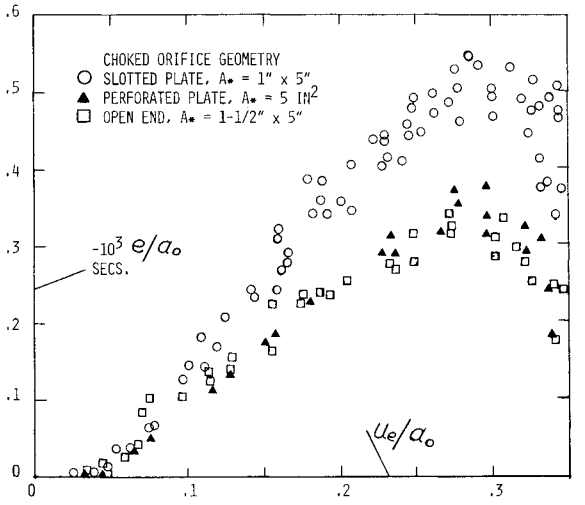

Fig. 5 Effect of choked orifice geometry on e **at 7 ft station.** $p_o =$ **85 PSI.**

In Fig. 1, e is the x-axis intercept of the straight characteristic through x,t and also represents the x displacement of the local particle at x,t from its equivalent position in a centered wave for a given velocity u_e. To any such point x,t there corresponds a unique value of e determined only by u_e, i.e., $(x-e)/t = (\gamma+1)u_e/2 - a_o$. Thus the noncentered flow is completely defined by specifying $e(u_e)$. For a centered wave $e \equiv o$. For a noncentered wave, e may be $\gtrless o$ in general, e.g., a constant acceleration piston gives $e > o$ for compression waves and $e < o$ for expansion waves. It can be shown[2] that not only e but also de/du_e must vanish at the wavehead. For experimental waves the function $e(u_e)$ can be determined from a single record of p vs t (or u_e vs t) at any x location.[2] It should be emphasized that e is a very sensitive quantity to so determine, and the present results for e contain appreciable scatter because of small differences in data from repeated experiments and random uncertainties or variations in reading the data.

Figure 3 shows e vs u_e determined from pressure histories measured at various stations along the tube (distances from diaphragm) for the conditions $p_o = 85$ psi, $T_o = 74.5°$F, and the orifice plate geometry a 1 in. × 5 in. rectangular slot. With this particular orifice plate the wave tail (or the beginning of the constant-property flow following the wave) occurs at $u_e/a_o = 0.367$ (local Mach number 0.398). The first feature to be noted in Fig. 3 is that that data from the different stations coalesce into one curve or grouping only after the wave has travelled a distance of the order of 5 to 7 ft along the tube. Because $e(u_e)$ must be independent of x for a strictly plane wave, this behavior suggests that the wave is initially nonplanar or curved from the three-dimensional effects present in its initial formation. Other features to be noted in Fig. 3 are that e is negative, so that p is less than the centered wave value, and that the magnitude of e passes through a maximum. These latter features were found to be typical for all conditions studied. In particular, the maximum in $|e|$ similarly occurs with no orifice plate (e.g., Fig. 5) and thus does not appear to be related to the finite extent of the wave (i.e., the wave tail location).

Figure 4 shows the measured speed of the wavehead intercept with the wall vs distance along the tube. The speed was determined from the time of passage of the wavehead over two closely spaced pressure transducers. For a plane wave the wavehead intercept speed should be the sound speed a_o. The measured speed exceeds a_o initially but decreases to a_o with distance along the tube. This behavior is interpreted as additional evidence that the wave is initially nonplanar.

The influence of orifice plate geometry is also illustrated in Fig. 4, and further in Fig. 5 which shows $e(u_e)$ determined from pressure data at the 7-ft station. In addition to the 1 in. × 5 in.

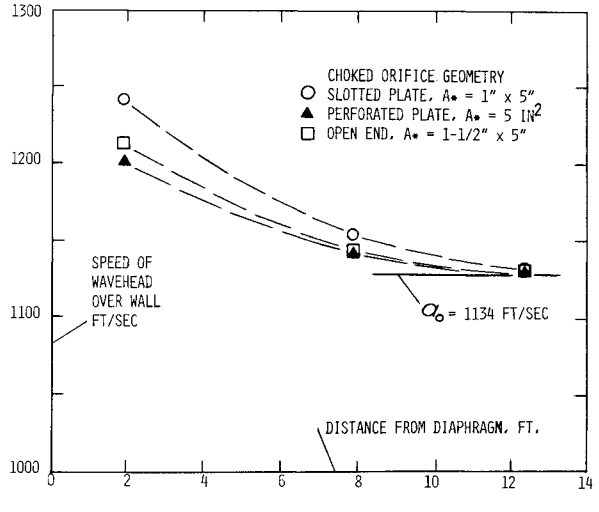

Fig. 4 Measured speed of wavehead intercept with wall. $p_o = 74$ **PSI,** $T_o = 74.5°$**F.**

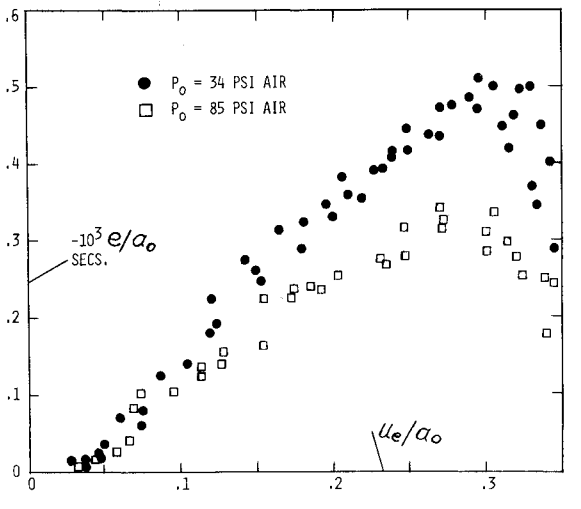

Fig. 6 Effect of p_o **on** e **at 7 ft station. Tube end fully open.**

rectangular slot orifice, two other tube end conditions were used: an orifice plate perforated with a uniform pattern of $\frac{1}{2}$-in. diam. holes giving a total orifice area $A_* = 5$ in.^{2}, and the condition of the tube end fully open with sonic flow at the exit ($A_* = 1\frac{1}{2}$ in. $\times$ 5 in.). The diaphragm configuration was identical for the three tube end conditions. The presence of an orifice plate appears to have limited effect on the waveform; the waveform for the perforated plate is essentially the same as for no orifice plate (Fig. 5).

Figure 6 shows the effect of reduced p_o on $e(u_e)$ determined at the 7-ft station for the tube end fully open. At the lower pressure level two different diaphragm materials were used: 0.001 in. mylar, which tends to tear on rupture; and 0.0003 in. "red-zip" cellophane, which shatters into small fragments on rupture. No measurable difference in waveform was observed for the two materials.

In conclusion, the present study shows diaphragm generated expansion waves to have wavehead first derivatives that are essentially discontinuous. A wavehead first derivative measured at any x then determines a unique x,t coordinate system. In that system, noncentered plane waves are conveniently described by the function $e(u_e)$ determinable from a measured pressure or velocity history at any x. It might be added that through e a *local* conical similarity exists for the inviscid noncentered wave[1,2] in terms of the similarity variable $S = 1 + x/a_o t - e/a_o t$.

References

[1] Hall, J. G., Srinivasan, G., and Rathi, J. S., "Laminar Boundary Layer in Noncentered Unsteady Waves," *AIAA Journal*, Vol. 11, No. 12, Dec. 1973, pp. 1770–1772.

[2] Hall, J. G., Srinivasan, G., and Rathi, J. S., "Analysis of Laminar Boundary Layers in Non-Centered Unsteady Waves," FTSL TR 73-1, Feb. 1973, Fluid and Thermal Sciences Lab., State University of New York at Buffalo, Buffalo, N.Y.

Ion Current Collection by Cylindrical Electrostatic Probe in a Flowing Plasma

KEIICHI KUSUMOTO,* TAKAO YOSHIKAWA,† AND TOSHIMITSU MURASAKI‡
Faculty of Engineering Science, Osaka University, Osaka, Japan

Nomenclature

e = electronic charge
i = ion current
$i_{\|}$ = ion current when probe axis is parallel to flow direction
k = Boltzmann constant
m_i = ion mass
n = electron number density
r_p = probe radius
T_e = electron temperature
T_i = ion temperature
U = flow speed
V = probe potential with respect to plasma
θ = angle between probe axis and flow direction
λ_D = Debye length, $(\varepsilon_o kT_e/e^2 n)^{1/2}$
λ_{ii} = ion-ion mean free path
λ_{in} = ion-neutral mean free path

Received November 2, 1973.
Index category: Plasma Dynamics and MHD.

* Graduate Student, Dept. of Mechanical Engineering.
† Assistant, Dept. of Mechanical Engineering.
‡ Professor, Dept. of Mechanical Engineering.

Introduction

THE behavior of cylindrical electrostatic probes in a flowing plasma are of substantial interest to those concerned with satellites, magneto-plasma-dynamic accelerators and high-temperature hypersonic wind tunnels. For such flow conditions, there are many aspects of electrostatic probe responses that remain unexplained. One of them is the effect of angle of incidence of the probe. In the intermediate values of probe radius to Debye length ratios ($0.1 < r_p/\lambda_D < 10$), Sonin[1] and Jakubowski[2] showed that an ion current peak occurred near zero angle of attack. In this Note, we present experimental results on ion current responses in a flowing plasma. Typical test conditions are as follows; $0.25 < T_i/T_e < 0.8$, $U/(kT_e/m_i)^{1/2} < 3.5$, $2 < r_p/\lambda_D < 200$. For the smallest radius probe, λ_{ii}/r_p ranged from 0.5 to 10 and λ_{in}/r_p was much larger than unity. In this range of parameters, if a sufficiently long cylindrical probe is directed along the stream, the response of the probe can be, in principle, interpreted within the framework of the theory of a stationary collisionless plasma.[3] However, the effect of the angle of incidence remains a substantial uncertainty,[1] because the potential distribution around the probe loses its symmetry and theoretical analyses are not made except for the special cases.[4,5]

Experimental Investigation

A d.c. arc jet was used as a plasma source. A supersonic plasma flow was obtained by being expanded from a Laval nozzle. Argon was used as the test gas. Details of this facility have been reported in Ref. 6.

The cylindrical probes used in this experiment were made of tungsten wire and their diameters ranged from 0.02 mm to 0.2 mm; the ratio of the probe length to the radius was larger than 100 except for the probe of 0.1 mm radius; the axial velocity of the flow was measured by the time-of-flight method to an accuracy of about 10%. The Mach number was obtained from the ratio of an impact and a static pressures, assuming the existence of a normal shock wave in front of the pitot-tube. The electron temperature and number density are evaluated from the current-voltage characteristic of the cylindrical probe which axis was parallel to the flow direction.

The influence of flow speed on an ion current was studied by turning the probe. Some examples of ion current variations are shown in Fig. 1 when the probe potential was held at a fixed value. In each case presented below, the dimensionless probe potential eV/kT_e was in the range of -20 to -30. It is found from Fig. 1 that typical probe responses of three kinds exist. In previous experiments,[1,2] the ion temperature was much smaller than the electron temperature and ion acoustic Mach number

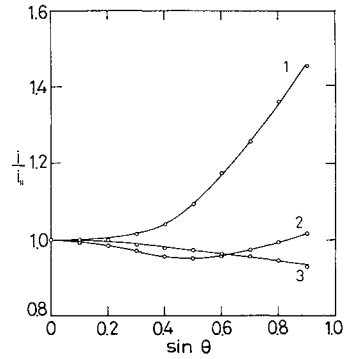

Fig. 1 Variation of ion current with probe orientation. 1) $r_p/\lambda_D = 69$, $r_p = 0.05$ mm, $U/(kT_e/m_i)^{1/2} = 3.5$, $T_i/T_e \approx 0.5$; 2) $r_p/\lambda_D = 150$, $r_p = 0.1$ mm, $U/(kT_e/m_i)^{1/2} = 2.2$, $T_i/T_e \approx 0.33$; 3) $r_p/\lambda_D = 4.4$, $r_p = 0.01$ mm, $U/(kT_e/m_i)^{1/2} = 1.3$, $T_i/T_e \approx 0.4$.